
HYBRID FOCAL AND FULL-RANGE ATTENTION BASED GRAPH TRANSFORMERS

Minhong Zhu

Department of Bioinformatics
School of Biology and Basic Medical Sciences
Soochow University, China

Zhenhao Zhao, Weiran Cai *

School of Computer Science
Soochow University, China

ABSTRACT

The paradigm of Transformers using the self-attention mechanism has manifested its advantage in learning graph-structured data. Yet, Graph Transformers are capable of modeling full range dependencies but are often deficient in extracting information from locality. A common practice is to utilize Message Passing Neural Networks (MPNNs) as an auxiliary to capture local information, which however are still inadequate for comprehending substructures. In this paper, we present a purely attention-based architecture, namely **Focal and Full-Range Graph Transformer (FFGT)**, which can mitigate the loss of local information in learning global correlations. The core component of FFGT is a new mechanism of compound attention, which combines the conventional full-range attention with K-hop focal attention on ego-nets to aggregate both global and local information. Beyond the scope of canonical Transformers, the FFGT has the merit of being more substructure-aware. Our approach enhances the performance of existing Graph Transformers on various open datasets, while achieves compatible SOTA performance on several Long-Range Graph Benchmark (LRGB) datasets even with a vanilla transformer. We further examine influential factors on the optimal focal length of attention via introducing a novel synthetic dataset based on SBM-PATTERN.

1 Introduction

Deep learning has shown its ability in modeling complex relationship in graph-structured data across diverse domains including chemistry, social science and biology. Facing the complex nature of data structure, the learning paradigm is under continuous evolution. The first surge of research interest was aroused by the message passing mechanism [1], where messages are aggregated and propagated through neighbouring nodes to capture local structural information. This paradigm of Message Passing Neural Network (MPNN) has been extensively validated for structural and semantic representations [2–4], yet has also revealed its shortcomings known as over-smoothing [5] and over-squashing [6, 7]. Inspired by the success of Transformers in natural language processing [8] and computer vision [9], the next generation of work has opened a new path in using self-attention mechanisms specifically for graph data, namely Graph Transformers (GTs). The key motivation is that by building long-range dependencies over the entire graph [10], this mechanism is endowed with more expressive power through a graph-level scope and mitigate the deficiencies of MPNNs [3].

Graph transformers are expected to comprehend structures across scales and the underlying semantic information. However, the lack of strong inductive bias [9] often makes the canonical Transformers struggle when applied to graph data. An effective way of retrieving structural information is to use positional encoding [11]. Models following this paradigm include leveraging absolute positional encoding [12, 13], pair-distance information [14, 15], graph kernels [16]. [17] summarizes a unified framework of this kind where positional encoding can be selectively added to one or multiple locations within input representations, attention and values. Notably, a prominent feature with GTs is the rich possibilities of incorporating edge information into the inductive bias [14, 15, 18, 19], which often helps to achieve SOTA performance [18, 19].

*Correspondance should be addressed to: wrcai@suda.edu.cn

However, GT models, proficient in establishing global dependencies, are still inadequate in the perception of local substructures that are often intrinsic to specific graph categories. An effective compound approach is to compensate GTs by utilizing modules to explicitly enhance information aggregation from locality. A common practice is utilizing MPNNs as an auxiliary to the global self-attention [20]. Existing methods include building Transformer blocks on top of MPNNs [21, 22], alternately stacking MPNN blocks and Transformer blocks [23], and parallelizing MPNN blocks and Transformer blocks [10, 24]. A typical example is GraphGPS [10] combining Transformer layers (with positional encoding) and MPNNs into a unified framework, which achieves SOTA performance. Yet, there still exist several flaws by utilizing MPNNs: (i) Using stacked MPNN modules is known to suffer from over-squashing and will lead to information loss. (ii) For substructures with a larger diameter (≥ 2), applying MPNN layer-wise will compromise the integrity of substructural information. (iii) Relying solely on MPNNs to process edge information is insufficient in extracting the relationship among nodes and edges [18].

In this work, we propose a purely attention-based architecture, the **Focal and Full-Range Graph Transformer (FFGT)**, which is proficient in acquiring both global and local information. A typical FFGT layer realizes an attention mechanism at different scales through two compensating modules: While the full-range attention module follows the canonical design of attention layer that acquire global correlations, it is compensated by a focal attention module that focuses on local ego-nets with a properly chosen receptive field. By hybridizing attention at different scales, the interaction between intrinsic local substructures and graph-level information can be effectively captured. While this compound mechanism enhances existing global attention-based GTs with the desirable substructure-awareness, it out-competes models based on limited receptive fields where access to graph-level information is not rendered, such as GT-Sparse [13] (only nearest neighbour nodes correlated), K-hop MPNN [25] (no acquisition of global information) and SAN [12] (low attention on distant nodes). Another crucial advantage of the proposed architecture is in the improved acquisition of local substructural information. Compared to convolution-based models such as K-hop MPNNs (will be discussed in Section 3, the focal attention module provides far more flexibility allowing exploration in a broader solution space. With the above mentioned two merits, the proposed framework can benefit us by correlating information at different scales through the compound attention mechanism, which may serve as an important perspective towards utilizing graph transformers.

The rest of the paper will include the following parts:

- We propose FFGT, a purely attention-based architecture that hybridizes the local substructural information of ego-nets and the global information over the entire graph. The architecture can be flexibly embodied by advanced attention techniques without increasing the complexity.
- We carry out extensive experiments on real-life benchmarks containing small-sized to large-sized graphs to evaluate the effectiveness of our approach. Even with simple attention modules adapted from a vanilla Transformer [8], our model can match or outperform SOTA methods on datasets from Long Range Graph Benchmark (LRGB) [26]
- We identify the importance of the intrinsic scale of substructures on different graphs. We design a new type of tests based on synthetic datasets generated with the Stochastic Block Model (SBM) [27] to illustrate how our model is able to identify such variation of substructures through the change of focal length.

2 Related Works

Graph Transformers with Improved Attention The success of Transformers in NLP and CV has spurred recent endeavors to craft specialized Transformers tailored for graph data. However, integrating structural information into the canonical Transformer architecture is not a straightforward task, owing to the intricate nature of graph structures. An effective strategy is to enhance attention computation by introducing supplementary structural information. Graphormer[14] adds spatial encoding and edge encoding to attention matrix to provide extra structural information. Such idea is further improved in GRPE [15] by introducing node-spatial and node-edge relations. In the recent work CSA [14], the attention module is enriched by Chromatic Self-Attention (CSA), which selectively modulates message channels between two nodes. Different from its predecessors, GRIT [19] employs virtual edge representations to compute the attention matrix representation. By iteratively updating the edge representation layer by layer, GRIT effectively amalgamates structural information with real edge information. Besides, some previous works treat both nodes and edges as tokens [28, 29] and theoretically result in the expressiveness boost.

MPNN-Auxiliary Graph Transformers Mounting MPNNs is another popular strategy to involve structural information in GTs. GraphTrans[18] adds Transformer blocks after standard GNN blocks, with the intention to enhance the local awareness gained from MPNNs. Mesh Graphormer [23] stacks a Graph Residual Block (GRB) on a Transformer layer to model both local and global interactions among 3D mesh vertices and body joints. The recent work GraphGPS

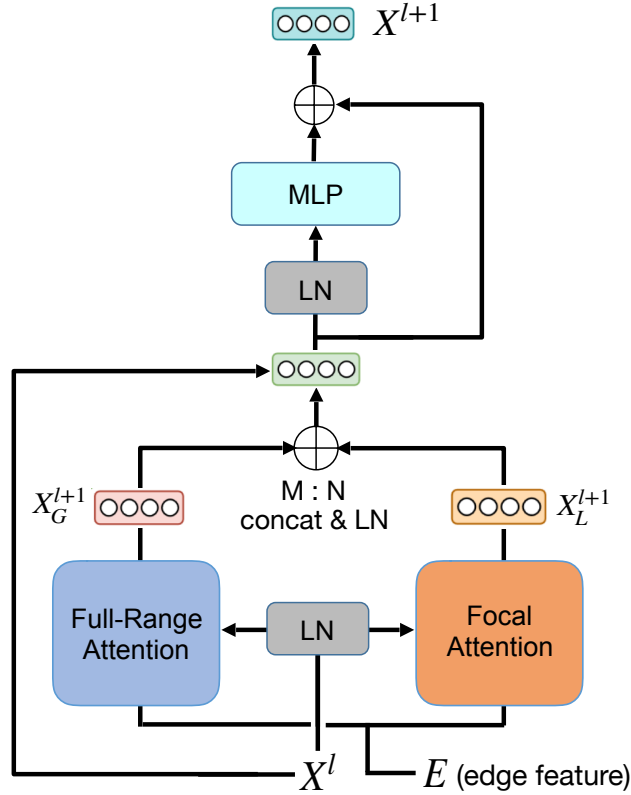


Figure 1: FFGT layer of compound attention consisted of compensating scopes: the full-range attention block is a fully-connected attention block for obtaining global correlations, while the focal attention block is an attention module delimited to local ego-nets for comprehending substructural information. Each attention block is comprised of a number of attention heads (M and N, respectively). The output of each layer is concatenated to allow integration from different scopes. Edge features are used by the two attention blocks separately.

[10] further improves the idea by providing a unified recipe for designing GTs. It integrates the MPNN-based models with global attention (with extra PE/SE) to enhance the model’s expressivity.

Subgraph GNNs Subgraph GNNs apply MPNNs to a set of subgraphs extracted from the input graph and aggregate the resulted representations in order to break the expressivity bottleneck of MPNNs. SubGNN [30] employs a message-passing framework to propagate messages from a set of anchor patches to the subgraph, enabling the capture of distinctive properties within the subgraph. SUN [31] unifies Subgraph GNN architectures and proves that they are bounded by 3-WL test. Another thread of work focuses on developing K-hop MPNNs [25] and promotes the expressivity by injecting substructural information [32]. Following the advances in subgraph-involving GNNs, the concept of subgraph-level modeling is integrated into Graph Transformers. Graph ViT/MLP-Mixer [33] leverages the ViT/MLP Mixer architecture introduced for CV by tokenizing subgraphs to achieve linear time/memory complexity. Similar ideas are adopted in work that attempts to scale GTs [34–36].

3 Methods

We propose a framework that integrates full-range attention over the entire graph and focal attention on local ego-nets. This framework has the merits of merging different scopes of attention, encapsulating much richer information of local substructures and mitigating over-smoothing and over-squashing brought by MPNNs. Moreover, the purely attention-based framework enables various ways of employing and updating edge information.

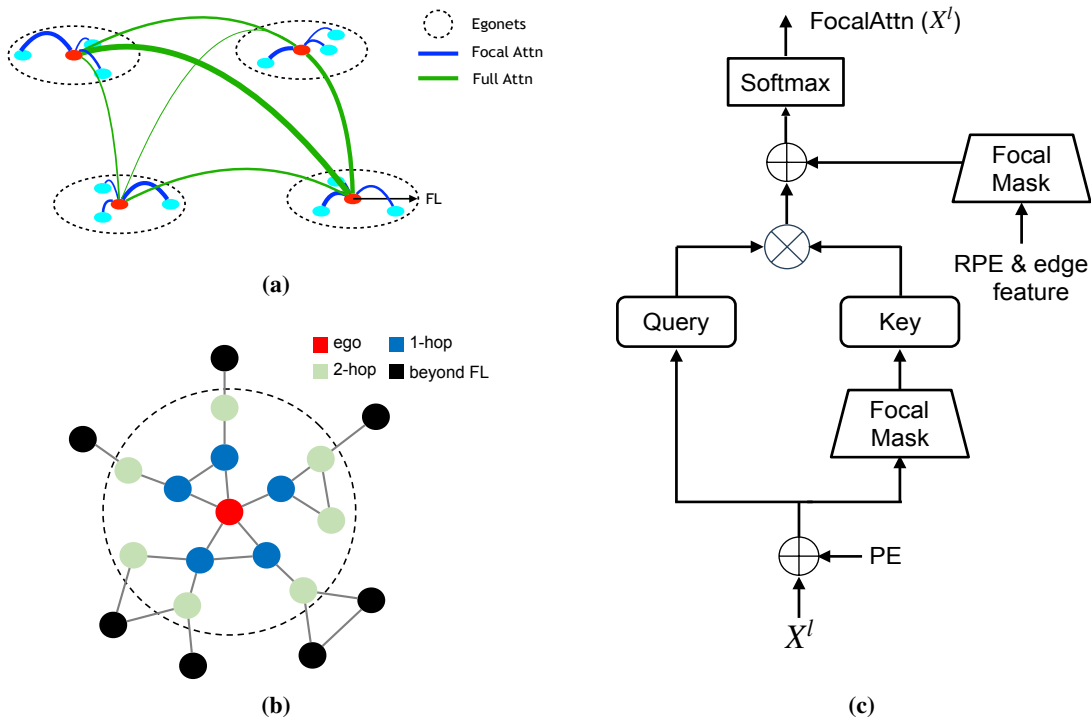


Figure 2: Focal Attention Block. (a) Focal Attention prunes high correlations over long ranges (green lines), allocating more focus to the locality (blue lines); (b) Example of a local ego-net with $FL = 2$. Nodes (black) outside the circle (i.e. with distance greater than 2 hops) are excluded from attention computation; (c) Detailed architecture inside the focal attention block. Focal Mask $FM \in \mathbb{R}^{n \times n}$ is employed to exclude nodes beyond the ego-net range, with $FM_{ij} = 1$ only when node j belongs to the K -hop ego-net centered on node i and $FM_{ij} = 0$ otherwise.

3.1 FFGT layer

Here we introduce the FFGT layer of compound attention. We first define the paradigm that can be instantiated with a general attention functionality and give a specific instantiation of the model in the next.

Paradigm of Compound Attention A standard FFGT layer consists of a full-range attention layer to capture global information and a focal attention layer to extract local substructural information. The full-range attention layer can be any unbounded fully connected attention layer, whereas the focal attention layer is allowed to employ another attention mechanism that is more proper for perceiving local substructures. Likewise, the ratio of the number of attention heads $M : N$ of both modules can be optimally set. The interaction of the two modules is rendered through aggregating the output of all attention heads. The architecture is illustrated in Fig. 1 (residual connections with layer normalization are omitted for clarity), which is formulated below

$$X^{l+1} = MLP(Aggr(X_G^{l+1}, X_L^{l+1})) \quad (1)$$

$$X_G^{l+1} = FullAttn(X^l) \quad (2)$$

$$X_L^{l+1} = FocalAttn(X^l) \quad (3)$$

where $FullAttn$ and $FocalAttn$ are instances of a global attention mechanism and a delimited attention mechanism with learnable parameters, respectively. $Aggr$ is the modular aggregation strategy, which can be realized by a concatenation function of all heads of both attention modules, followed by a linear layer further merging them; MLP is a 2-layered MLP block.

Focal Attention To establish auxiliary local information representation of subgraphs, we deploy multiple heads for attention of a delimited range in a GT. A K-hop ego-net centered at each node is extracted on which the focal attention with a local inductive bias is used to explore the nodal correlations (Fig. 2a). The node representation can be updated as follows

$$X_i = \sum_{j \in Ego\{i, FL=k\}} Attn(i, j | local\ bias) V_j \quad (4)$$

where $Ego\{i, FL = k\}$ refers to the K-hop ego-net rooted on node i ; $Attn(i, j)$ is the attention score between node i and node j ; V_j is the value of node j . The scale of the ego-net is defined by the focal length (FL), a hyperparameter critically related to the intrinsic substructure of the studied graph.

The superiority of focal attention in capturing local information can be expected with the comparison to K-hop MPNNs [25, 37]. The commonality between the two lies in the fact that with both, the root node receives messages from all nodes within its K-hop ego-net. However, with the K-hop MPNN, the same learnable weights are shared in aggregating local information at the same distance. In contrast, each focal attention head can take advantage of the nodes' relative distances as a bias and learns a pattern for aggregating message from all nodes within the ego-net. The latter enjoys full flexibility in treating the local network, benefited from relaxing largely the limitation of MPNNs in the aggregation, which is bounded by the requirement of invariance in the aggregating order. This means that only when the same attention weights are allocated to the nodes at the same distance, the functionality of focal attention degenerates to a K-hop MPNN layer. Therefore, the focal attention, by exploring a greater space of solutions, will be more powerful than K-hop MPNNs, which promises its ability in capturing local information.

3.2 Instantiation

The FFGT is highly flexible allowing independent selection of the attention mechanism used for attention modules of different scopes. Despite the choices, we demonstrate here how to embed the attention mechanisms in our architecture that are most commonly used in GTs, following the paradigm proposed in AutoGT [17]. To be specific, we compute the attention map as follows

$$Q = XW_Q, \quad K = XW_K \quad (5)$$

$$Attn(X) = softmax\left(\frac{QK^T}{\sqrt{d}} + B\right) \odot C \quad (6)$$

where $W_Q \in \mathbb{R}^{d \times d}$ and $W_K \in \mathbb{R}^{d \times d}$ are trainable parameters for queries and keys. Matrix $B \in \mathbb{R}^{n \times n}$ is the attention bias generally composed of the combination of relative positional encoding (RPE) [14, 15, 38] and edge features [14, 15]. $C \in \mathbb{R}^{n \times n}$ is an optional gate to enhance the relative positional encoding [39]. For those requiring absolute positional encoding, the node input can be augmented by positional encoding (PE) prior to entering the attention layer.

The delimited attention in focal attention layer is achieved through the *FocalMask* function applied to the keys, RPE and edge features, as shown in Fig. 2c. *FocalMask* is a binary matrix consisting of 0 and 1, which excludes nodes beyond the ego-net range from the attention computation. In comparison to using an Attention Mask [40], the advantage of employing *FocalMask* lies in its omission of correlation calculations involving the center node and nodes outside its ego-net. This enables the reduction of computation from quadratic complexity to a constant complexity, and thus does not alter the scalability. Formally, the focal attention module can be expressed as follows

$$Attn(X) = softmax\left(\frac{Q \times FM(K)^T}{\sqrt{d}} + FM(B)\right) \odot C \quad (7)$$

where FM is the Focal Mask function, which is a $\mathbb{R}^{n \times n}$ matrix with $FM_{ij} = 1$ if $j \in Ego(i, FL = K)$ and $FM_{ij} = 0$ otherwise.

Table 1: Comparison of FFGT with fully-connected GTs. Results are averaged over 4 runs with 4 different seeds.

Model	ZINC	MolPCBA	Peptides-func	Peptides-struct
	MAE↓	AP↑	AP↑	MAE↓
VANILLA	0.156±0.006	0.2638±0.0058	0.6648±0.0087	0.2500±0.0027
VANILLA-FFGT	0.140±0.005	0.2779±0.0049	0.6914±0.0040	0.2456±0.0017
GRPE	0.101±0.006	0.2856±0.0039	0.6836±0.0060	0.2422±0.0012
GRPE-FFGT	0.093±0.004	0.2902±0.0010	0.6956±0.0080	0.2416±0.0026

4 Experiments

4.1 Implementation Details

FFGT Attention Module Considering the composition of FFGT attention modules, one simple choice is to let the focal layer share the same correlation attention mechanism of full-range but within the focal range, although the choice of a distinct function may meet further needs. Here, we use this simplification and choose mechanisms used in Vanilla Transformer and GRPE to construct Vanilla-FFGT and GRPE-FFGT, respectively. By incorporating Vanilla Transformer, we are interested in testing how well the hybridization of Focal and Full-Range attention alone can benefit the learning, in spite of many alternatives. We also choose the more sophisticated GRPE because it involves a combination of RPE and Edge Encoding as attention bias, which can serve to examine our framework when effective inductive biases are introduced.

In the Vanilla-FFGT, we follow the Transformer+LapPE architecture proposed in [26]. Although the architecture in [26] does not involve edge information, we add edge encoding as attention bias for fair comparison. In GRPE-FFGT, we directly utilize the attention mechanism with edge features as used in the original.

Virtual Node For graph-level prediction tasks, following Graphormer, we adopt a special node called virtual node. It is connected to all real nodes in both full-Range and focal attention modules, which acts as a classification token [41].

4.2 Results on Graph Benchmarks

We primarily focus on evaluating the performance of the FFGT on graph-level tasks, where both local and global information is generally influential. Two small molecule benchmarks and two benchmarks from Long Range Graph Benchmarks are chosen. The former pair of benchmarks centers on small graphs where local information plays a pivotal role, while the latter pair is tailored for gauging a model’s ability of learning long-range dependencies. First, we compare FFGT with their backbone models separately on the 4 benchmarks. Then, we compare Vanilla-FFGT and GRPE-FFGT with the baselines containing SOTA Graph Transformer models and other GNN-based models. For completeness, we further conduct extra evaluations on node-level tasks to demonstrate the effectiveness of FFGT in capturing local information in various graph types. Details concerning experimental setups are provided in Appendix A.

Molecule Property Prediction We first evaluate FFGT on two small molecule datasets, ZINC from Benchmarking GNNs [27] and ogbg-MolPCBA from Open Graph Benchmark (OGB) [42]. As is shown in Table 1, FFGT promotes the performance on both small molecule benchmarks. The results demonstrate that in small molecule data sets where local information plays an important role, it is beneficial to employ global attention in alliance with focal attention as to mitigate the shortcomings of the former in understanding local substructures. On the ZINC dataset, we observe that the FFGT achieves the best performance when the focal length is set to 1, which aligns with the advantage of integrating a local MPNN with global attention as illustrated in GraphGPS. Nevertheless, interestingly, despite the similar average graph size, the optimal focal length for MolPCBA equals to 3. Such offset indicates that considering subgraphs beyond 1-hop neighbourhood is beneficial to identify the heterogeneity among graphs due to the detailed substructures.

Long Range Graph Benchmark(LRGB) We further evaluate the FFGT architecture on peptide-functional and peptide-structural datasets from LRGB. They are intended to test the model’s ability to capture long-range dependencies in the graph. As shown in Table 1, FFGT enhances the performance of the two backbone models on both datasets with statistical significance. A remark for Peptides-struct is that the structural properties to predict are primarily associated

Table 2: Comparison of FFGT with SOTA GTs and GNN-based models. We use "-" for missing values from literatures, bold for the best performance, and underlines for those where FFGT are compatible with the best models. Results are averaged over 4 runs with 4 different seeds

Model	ZINC	MolPCBA	Peptides-func	Peptides-struct
	MAE↓	AP↑	AP↑	MAE↓
GCN	0.226±0.014	0.2424±0.0034	0.5930±0.0023	0.3234±0.0006
GatedGCN	0.226±0.014	0.2670±0.0020	0.5864±0.0077	0.3420±0.0013
SUN	0.084±0.002	-	0.6730±0.0078	0.2498±0.0008
SAN + LapPE	0.139±0.006	0.2765±0.0042	0.6384±0.0121	0.2683±0.0042
GPS	0.070±0.004	0.2907±0.0028	0.6535±0.0041	0.2500±0.0012
Exphormer	-	-	0.6527±0.0043	0.2481±0.0007
MGT	0.131±0.003	-	0.6817±0.0064	0.2453±0.0025
Graph ViT	0.085±0.005	-	0.6942±0.0075	0.2449±0.0016
VANILLA-FFGT	0.140±0.005	0.2779±0.0049	<u>0.6914±0.0040</u>	<u>0.2456±0.0017</u>
GRPE-FFGT	0.093±0.004	<u>0.2902±0.0010</u>	0.6956±0.0080	0.2416±0.0026

with the relative positioning of atoms, and therefore GRPE with its relative positional encoding has sufficed to achieve exceptional performance.

Model Comparison We compare the FFGT with the state-of-the-art GTs and GNN-based models. The selection of baselines is intended to examine the effectiveness of FFGT. We use MPNNs and Subgraph GNNs (GCN [2], GatedGCN [43], SUN [31]) to show the necessity of global information. SAN [12] is a Graph Transformer largely limited to the neighbourhood, but puts emphasis on the role of full-range attention as well. GraphGPS [10] and Exphormer [35] hybrids Transformer and MPNNs, which are suitable to demonstrate when focal attention would be needed. Finally, Graph ViT [33] and MGT [36] implements coarsening-related strategies to learn subgraph-level representations, which contrasts with ours in acquiring information from substructures.

The results are shown in Table 2. We observe that the FFGT models surpass baselines significantly on two benchmarks from LRGB. Yet, although witnessing significant improvement compared to the backbone model, its performance is not better than or even inferior compared to some of the baselines in ZINC and Molpcba. It should be noted that such a gap generally comes from the nature of the datasets. In ZINC and Molpcba where local information matters more than global information, precise prediction largely depends on the comprehension of fine-grained local substructures. This is supported by the ablation studies with GraphGPS [10] where MPNN+PE is already able to achieve an excellent performance, whereas a Transformer module plays a very limited role. Since GRPE and Vanilla Transformer (without FFGT) largely underperform by themselves on the two datasets, it is hard to fill the gap with SOTA models by simply using FFGT, even with a significant boost. Using a stronger backbone models with the aid of FFGT may achieve a compatible or even surpassing result.

Node Classification For completeness, we test the FFGT architecture on node classification tasks to further illustrate its ability in comprehending local information. We use homophily Citation Networks (Cora, Citeseer) and heterophily Wikipedia Network (Chameleon) for evaluation. The performance is compared with Graph Transformers originally designed for graph-level tasks (SAN, Graphormer), and with those designed specifically for node-classification tasks (UniMP [44], NaGphormer [34]). Detailed descriptions of the datasets are shown in A.

Although not designed to tackle node-level problems, FFGT still improves the performance of GRPE on all datasets significantly, which demonstrates its ability to enhance local information capturing on various graph data. Without additional modifications in the attention mechanism, GRPE-FFGT can already out-perform UniMP and NaGphormer, which were specifically designed for node classification tasks. It is fair to note that GNNs usually performs better on these node-level tasks than Graph Transformers.

Table 3: Evaluation of FFGT on node-level tasks. We use "-" for the missing values from literature, bold for the best performance, and underlines for those where FFGT is compatible with the best baselines.

Model	Cora	CiteSeer	Chameleon
	Acc.(%) \uparrow	Acc.(%) \uparrow	Acc.(%) \uparrow
SAN	81.91 \pm 3.42	69.63 \pm 3.76	55.62 \pm 0.43
Graphormer	67.71 \pm 0.78	73.30 \pm 1.48	36.81 \pm 1.69
UniMP	84.18 \pm 1.39	75.00 \pm 1.59	-
NAGphormer	85.77 \pm 1.35	73.69 \pm 1.48	-
GRPE	82.52 \pm 1.30	72.59 \pm 1.40	54.65 \pm 1.50
GRPE-FFGT	86.59\pm0.83	75.31\pm1.32	62.52\pm0.97
Δ Acc-FFGT	+ 4.07	+ 2.72	+ 7.87

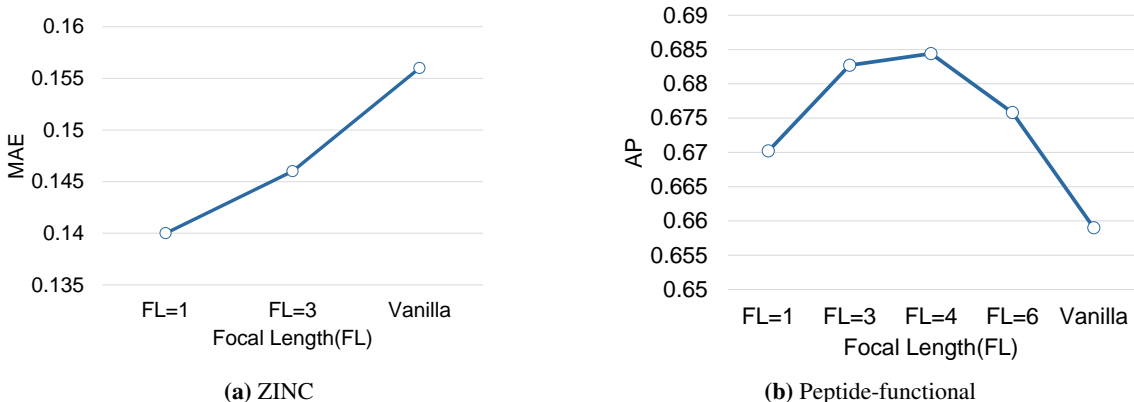


Figure 3: Ablation study of focal length (FL) on ZINC and Peptide-functional. Vanilla-FFGT is used as training model. The x-axis represents the focal length (FL), where vanilla refers to the fully-connected version

4.3 Ablation Study and Substructural Awareness

Substructures play an important role in real-world graph data, including functional groups in small molecules, amino acid residues in peptides, and communities in social networks. One major difficulty in learning these substructures is that their scales can vary greatly. Scale here refers to the measurement of how distant nodes within a substructure are with each other (e.g. average shortest path distance). In the following section, we explore the optimal choice of focal length in different types of graphs, and illustrate that compared to backbone models, FFGT can effectively capture the varying scales of key substructures.

4.3.1 Tests on Empirical Datasets

We evaluate the effect of different choices of FL on two empirical datasets: ZINC and Peptide-functional. For small molecules in ZINC, important functional groups usually contains only 3-5 atoms (e.g. carboxyl and aldehyde groups), with Multivariate ring (e.g. benzene ring) as exception. Conversely, the key substructures in peptides in Peptide-functional are amino acid residues, which can have up to 14 atoms in their side chains. This indicates that the scales of the substructures in the two datasets differ significantly.

Figure 3 shows the ablation results. We refer to $FL = 0$ as Vanilla which represents the raw backbone model. For ZINC, the best performance is reached at $FL = 1$; in contrast, for Peptide-functional, the performance peaks at $FL = 4$. It is very enlightening that the maximum number of carbon atoms in the side chain of amino acids is 4, which means that it takes 4 hops for alpha carbon atoms to "see" all the main atoms of the side chains. This indicates that focal

Table 4: Performance of VANILLA-FFGT on different SBM-Pattern datasets as FL varies. Results are averaged over 8 runs.

Model	p=0.16	p=0.14	p=0.12	p=0.10
Vanilla	87.3625±0.0699	84.2871±0.0729	81.3535±0.0650	78.9624±0.0378
$FL = 1$	87.6101±0.0995	84.4141±0.0406	81.4364±0.0634	78.9674±0.0464
$FL = 2$	87.4651±0.0843	84.3915±0.0688	81.4489±0.0426	79.0464±0.0435
$FL = 3$	87.4412±0.0709	84.3270±0.0567	81.4277±0.0745	79.0292±0.0564

attention can learn such characteristic of amino acid, while a performance decrease when $FL > 4$ indicates a lack of recognition of such key substructures in purely attention setting. As for ZINC, $FL = 1$ is already sufficient for central atoms in most functional groups to "see" each other. The above results show that the optimal focal length in FFGT is highly correlated with the scale of the substructure on the graph.

4.3.2 Controlled Tests on SBM-PATTERN

Results from the ablation studies on empirical datasets show significant variations in the optimal focal length between different graphs, as well as strong correlation with the size of important substructures. To further explore the model’s ability to distinguish such characteristic of substructure, we choose to examine the dependence of the optimal FL explicitly on the adjustable community structures in a graph. More concretely, we adapt SBM-PATTERN, a synthetic dataset focusing on inductive node prediction, generated by the Stochastic Block Model (SBM), to create graphs with tunable scales of communities.

SBM-PATTERN PATTERN is the graph pattern recognition task presented in [45], aiming at finding a fixed graph pattern P embedded in a larger graph G (with pre-defined communities) of variable sizes. Later, a dataset based on the PATTERN task was introduced in [27], namely SBM-PATTERN. Graphs in SBM-PATTERN are generated using Stochastic Block Model (SBM), with parameter p be the intra-community edge probability, p_p the intra-pattern edge probability, q inter-community edge probability, q_p the community-pattern edge probability. By changing p , one can modify the scale of communities (the substructure here). This makes SBM-PATTERN suitable to observe the behaviour of FFGT when the scale of substructure varies.

Here we follow the same routine as in [27], but generate sparser graphs by setting q to 0.01 and q_p to 0.05. With these two probabilities fixed, we create 4 different datasets with different p and p_p , i.e. $p = p_p \in \{0.10, 0.12, 0.14, 0.16\}$. When p increases, it only extends the scale of communities without interfering connections between different communities and the pattern. Thus, the datasets generated from a larger p will have communities sharing a smaller scale. Under this setting, we can test if the scale of the local sub-structures (communities) has a close relation with the optimal FL . See Appendix B for detailed description and parameter settings.

Analyses of Results We train the Vanilla-FFGT with different FL s for 8 different random seeds on each datasets, as is shown in Table 4. The results show that when the community scale is small ($p = 0.16$), the model with $FL = 1$ performs the best with a statistical significance. As the community scale extends ($p = 0.14, 0.12$), the model with $FL = 2$ performs on par with that with $FL = 1$. When the scale of the community reaches a certain extent ($p = 0.10$), the model with $FL = 2$ outperforms that with $FL = 1$ with a statistical significance (comparable with $FL = 3$). At the same time, the backbone model always perform the worst. We can conclude from this trend that there is a significant correlation between the optimal FL and the scale of the local community. Together with findings in Empirical datasets, we can conclude that FFGT is able to be more aware of the intrinsic scale of substructures compared with backbone models.

5 Conclusion

We propose a framework that integrates full-range attention, which focuses on global information, and focal attention, which specializes in local substructure information, in order to mitigate the deficiency of the Graph Transformer in acquiring local information. Unlike previous efforts that supplemented local information using MPNNs, the focal attention module we employ overcomes the information loss introduced by stacking layers of MPNNs and can attain more comprehensive information about local substructures. Experimental results on graph datasets of different scales

demonstrate the effectiveness of our framework, as even with a simple backbone model, it can rival SOTA performance. And a synthetic experiment illustrates that our framework can adapt to variations in the range of substructures within graph data. Given the high flexibility of our framework, there are numerous avenues for further exploration in the future. These include linearization of full-range attention module, refining the design of the focal attention module, and employing better methods for utilizing edge information.

References

- [1] Justin Gilmer et al. “Neural message passing for quantum chemistry”. In: *International conference on machine learning*. PMLR. 2017, pp. 1263–1272.
- [2] Thomas N Kipf and Max Welling. “Semi-supervised classification with graph convolutional networks”. In: *arXiv preprint arXiv:1609.02907* (2016).
- [3] Keyulu Xu et al. “How powerful are graph neural networks?” In: *arXiv preprint arXiv:1810.00826* (2018).
- [4] Petar Veličković et al. “Graph attention networks”. In: *arXiv preprint arXiv:1710.10903* (2017).
- [5] Qimai Li, Zhichao Han, and Xiao-Ming Wu. “Deeper insights into graph convolutional networks for semi-supervised learning”. In: *Proceedings of the AAAI conference on artificial intelligence*. Vol. 32. 1. 2018.
- [6] Uri Alon and Eran Yahav. “On the bottleneck of graph neural networks and its practical implications”. In: *arXiv preprint arXiv:2006.05205* (2020).
- [7] Jake Topping et al. “Understanding over-squashing and bottlenecks on graphs via curvature”. In: *arXiv preprint arXiv:2111.14522* (2021).
- [8] Ashish Vaswani et al. “Attention is all you need”. In: *Advances in neural information processing systems* 30 (2017).
- [9] Alexey Dosovitskiy et al. “An image is worth 16x16 words: Transformers for image recognition at scale”. In: *arXiv preprint arXiv:2010.11929* (2020).
- [10] Ladislav Rampášek et al. “Recipe for a general, powerful, scalable graph transformer”. In: *Advances in Neural Information Processing Systems* 35 (2022), pp. 14501–14515.
- [11] Luis Müller et al. “Attending to graph transformers”. In: *arXiv preprint arXiv:2302.04181* (2023).
- [12] Devin Kreuzer et al. “Rethinking graph transformers with spectral attention”. In: *Advances in Neural Information Processing Systems* 34 (2021), pp. 21618–21629.
- [13] Vijay Prakash Dwivedi and Xavier Bresson. “A generalization of transformer networks to graphs”. In: *arXiv preprint arXiv:2012.09699* (2020).
- [14] Chengxuan Ying et al. “Do transformers really perform badly for graph representation?” In: *Advances in Neural Information Processing Systems* 34 (2021), pp. 28877–28888.
- [15] Wonpyo Park et al. “Grpe: Relative positional encoding for graph transformer”. In: *arXiv preprint arXiv:2201.12787* (2022).
- [16] Grégoire Mialon et al. “Graphit: Encoding graph structure in transformers”. In: *arXiv preprint arXiv:2106.05667* (2021).
- [17] Zizhao Zhang et al. “Autogt: Automated graph transformer architecture search”. In: *The Eleventh International Conference on Learning Representations*. 2022.
- [18] Zhe Chen et al. “Graph Propagation Transformer for Graph Representation Learning”. In: *arXiv preprint arXiv:2305.11424* (2023).
- [19] Liheng Ma et al. “Graph Inductive Biases in Transformers without Message Passing”. In: *arXiv preprint arXiv:2305.17589* (2023).
- [20] Erxue Min et al. “Transformer for graphs: An overview from architecture perspective”. In: *arXiv preprint arXiv:2202.08455* (2022).
- [21] Zhanghao Wu et al. “Representing long-range context for graph neural networks with global attention”. In: *Advances in Neural Information Processing Systems* 34 (2021), pp. 13266–13279.
- [22] Yu Rong et al. “Self-supervised graph transformer on large-scale molecular data”. In: *Advances in Neural Information Processing Systems* 33 (2020), pp. 12559–12571.
- [23] Kevin Lin, Lijuan Wang, and Zicheng Liu. “Mesh graphormer”. In: *Proceedings of the IEEE/CVF international conference on computer vision*. 2021, pp. 12939–12948.
- [24] Jiawei Zhang et al. “Graph-bert: Only attention is needed for learning graph representations”. In: *arXiv preprint arXiv:2001.05140* (2020).
- [25] Giannis Nikolentzos, George Dasoulas, and Michalis Vazirgiannis. “k-hop graph neural networks”. In: *Neural Networks* 130 (2020), pp. 195–205.

- [26] Vijay Prakash Dwivedi et al. “Long range graph benchmark”. In: *Advances in Neural Information Processing Systems* 35 (2022), pp. 22326–22340.
- [27] Vijay Prakash Dwivedi et al. “Benchmarking graph neural networks”. In: *arXiv preprint arXiv:2003.00982* (2020).
- [28] Md Shamim Hussain, Mohammed J Zaki, and Dharmashankar Subramanian. “Global self-attention as a replacement for graph convolution”. In: *Proceedings of the 28th ACM SIGKDD Conference on Knowledge Discovery and Data Mining*. 2022, pp. 655–665.
- [29] Jinwoo Kim et al. “Pure transformers are powerful graph learners”. In: *Advances in Neural Information Processing Systems* 35 (2022), pp. 14582–14595.
- [30] Emily Alsentzer et al. “Subgraph neural networks”. In: *Advances in Neural Information Processing Systems* 33 (2020), pp. 8017–8029.
- [31] Fabrizio Frasca et al. “Understanding and extending subgraph gnn’s by rethinking their symmetries”. In: *Advances in Neural Information Processing Systems* 35 (2022), pp. 31376–31390.
- [32] Jiarui Feng et al. “How powerful are k-hop message passing graph neural networks”. In: *Advances in Neural Information Processing Systems* 35 (2022), pp. 4776–4790.
- [33] Xiaoxin He et al. “A generalization of vit/mlp-mixer to graphs”. In: *International Conference on Machine Learning*. PMLR. 2023, pp. 12724–12745.
- [34] Jinsong Chen et al. “NAGphormer: A tokenized graph transformer for node classification in large graphs”. In: *The Eleventh International Conference on Learning Representations*. 2022.
- [35] Hamed Shirzad et al. “Expformer: Sparse transformers for graphs”. In: *arXiv preprint arXiv:2303.06147* (2023).
- [36] Nhat Khang Ngo, Truong Son Hy, and Risi Kondor. “Multiresolution graph transformers and wavelet positional encoding for learning long-range and hierarchical structures”. In: *The Journal of Chemical Physics* 159.3 (2023).
- [37] Tianjun Yao et al. “Improving the Expressiveness of K-hop Message-Passing GNNs by Injecting Contextualized Substructure Information”. In: *Proceedings of the 29th ACM SIGKDD Conference on Knowledge Discovery and Data Mining*. 2023, pp. 3070–3081.
- [38] Jianan Zhao et al. “Gophormer: Ego-graph transformer for node classification”. In: *arXiv preprint arXiv:2110.13094* (2021).
- [39] Shengjie Luo et al. “Your transformer may not be as powerful as you expect”. In: *Advances in Neural Information Processing Systems* 35 (2022), pp. 4301–4315.
- [40] Erxue Min et al. “Masked transformer for neighbourhood-aware click-through rate prediction”. In: *arXiv preprint arXiv:2201.13311* (2022).
- [41] Jacob Devlin et al. “Bert: Pre-training of deep bidirectional transformers for language understanding”. In: *arXiv preprint arXiv:1810.04805* (2018).
- [42] Weihua Hu et al. “Open graph benchmark: Datasets for machine learning on graphs”. In: *Advances in neural information processing systems* 33 (2020), pp. 22118–22133.
- [43] Xavier Bresson and Thomas Laurent. “Residual gated graph convnets”. In: *arXiv preprint arXiv:1711.07553* (2017).
- [44] Yunsheng Shi et al. “Masked label prediction: Unified message passing model for semi-supervised classification”. In: *arXiv preprint arXiv:2009.03509* (2020).
- [45] Franco Scarselli et al. “The graph neural network model”. In: *IEEE transactions on neural networks* 20.1 (2008), pp. 61–80.
- [46] Prithviraj Sen et al. “Collective classification in network data”. In: *AI magazine* 29.3 (2008), pp. 93–93.
- [47] Hongbin Pei et al. “Geom-gcn: Geometric graph convolutional networks”. In: *arXiv preprint arXiv:2002.05287* (2020).
- [48] Benedek Rozemberczki, Carl Allen, and Rik Sarkar. “Multi-scale attributed node embedding”. In: *Journal of Complex Networks* 9.2 (2021), cnab014.
- [49] Ilya Loshchilov and Frank Hutter. “Decoupled weight decay regularization”. In: *arXiv preprint arXiv:1711.05101* (2017).

A Empirical Datasets

The FFGT is evaluated on several graph-level and node-level empirical graph benchmarks.

A.1 Graph-level Datasets

Table 5: Statistics of graph-level datasets

Dataset	#Graphs	Avg.#nodes	Avg.#edges	Task	Metric
ZINC	12000	23.2	24.9	regression	MAE
MolPCBA	437,929	26.0	28.1	10-task classification	AP
Peptides-func	15,535	150.94	307.30	10-task classification	AP
Peptides-struct	15,535	150.94	307.30	11-task regression	MAE

ZINC [27] consists of $12K$ molecular graphs from the ZINC database of commercially available chemical compounds. These molecular graphs are between 9 and 37 nodes large. Each node represents a heavy atom (28 possible atom types) and each edge represents a bond (3 possible types). The task is to regress constrained solubility ($\log P$) of the molecule. The dataset comes with a predefined $10K/1K/1K$ train/validation/test split. The evaluation metric used is Mean Absolute Error (MAE).

ogbg-molpcba [42] is a molecular property prediction dataset adopted by OGB from MoleculeNet. It is derived from PubChem BioAssay, targets to predict results of 128 bioassays in multi-task binary classification setting. The evaluation metric used is Average Precision (AP).

Peptides-func [26] is composed of atom graphs derived from peptides retrieved from SATPdb. It contains $\sim 15k$ graphs with ~ 150 nodes per graph. It is targeted to predict 10 functions of peptides in multi-task binary classification setting, with average precision (AP) as the evaluation metric.

Peptides-struct [26] shares the same graph as Peptide-functional, but the task is graph regression of 11 3D structural properties of peptides, with Mean Absolute Error (MAE) as the evaluation metric.

A.2 Node-level Datasets

Table 6: Statistics of node-level datasets

Dataset	#Graphs	#Nodes	#edges	Task	Metric
Cora	1	2708	5429	7-classes classification	Accuracy
CiteSeer	1	3327	4732	6-classes classification	Accuracy
Chameleon	1	2277	36101	5-classes classification	Accuracy

Cora, CiteSeer [46] Cora and Citeseer are standard citation network benchmark datasets. In these networks, nodes represent papers, and edges denote citations of one paper by another. Node features are the bag-of-words representation of papers, and node label is the academic topic of a paper. We follow the $48/32/20$ split strategy proposed by [47]

Chameleon [48] Chameleon is a page-page network on specific topics in Wikipedia. In the dataset, nodes represent web pages and edges are mutual links between pages. And node features correspond to several informative nouns in the Wikipedia pages. We classify the nodes into five categories in term of the number of the average monthly traffic of the web page. The dataset is randomly split as $60/20/20$ for train/val/test. Results are averaged for 10 different splits.

B SBM-PATTERN

The original SBM-PATTERN dataset [27] considers node-level task of graph pattern recognition proposed in [45], which aims at finding a fixed graph pattern P embedded in larger graphs G of variable sizes. The graphs are generated with the Stochastic Block Model (SBM), which is widely used to model communities in social networks by modulating the intra- and extra-communities connections, thereby controlling the difficulty of the task. A SBM is a random graph generator which assigns communities to each node as follows: any two vertices are connected with the probability p if they belong to the same community, or they are connected with the probability q if they belong to different communities (the value of q acts as the noise level). The original SBM-Pattern generates graph with 5 communities and then embed 1 pattern into the graph.

The method of generating datasets using SBM-PATTERN is suitable for us to create new datasets to investigate how the scale of local substructure impact the choice of focal length (FL) in FFGT, for the following reasons: (i) In order to ascertain the specific attribution of nodes, the model needs to not only comprehensively grasp the substructural characteristics of the community in which the nodes are located, but also capture information from distant nodes. This aligns with the applicable scenarios of FFGT. (ii) By adjusting p and q , it is possible to generate graphs with arbitrary sparsity and control the scale of each community, which is the requirement for the experiment.

Table 7: Statistics of 4 SBM-PATTERN Datasets

Probability	#Graphs	Avg.#nodes	Avg.#degrees	Avg.#diameters
$p = 0.16$	12000	125	6.13	6.15
$p = 0.14$	12000	127	5.72	6.38
$p = 0.12$	12000	129	5.34	6.60
$p = 0.10$	12000	130	4.85	7.00

Following the setting in [27], we generate 4 different datasets with different scales of communities. A typical graph G is generated with 5 communities with size randomly selected between [5, 35]. The extra-probability q for each community is fixed to 0.01, with intra-probability $p \in \{0.10, 0.12, 0.14, 0.16\}$ varying among 4 datasets. We randomly generate 100 patterns P composed of 20 nodes with fixed extra-probability $q_p = 0.05$ (i.e., 5 % of nodes in P are connected to G) and intra-probability $p = p_p$. These 100 patterns are randomly assigned to the dataset, with each graph embedding one pattern. The node features on G are generated with a uniform random distribution with a vocabulary of size 3, i.e. $\{0, 1, 2\}$. The node features for P are also generated as a random signal with values $\{0, 1, 2\}$. The graphs are of sizes 44 – 188 nodes. The output node labels have value 1 if the node belongs to P and value 0 if it is in G . Each Datasets has 10,000 train, 2,000 validation, 2,000 test graphs. Statistics are shown in Table 7, when p increases, the graphs are sparsified and the scale of local community increases.

C Model Setting

Models used on experiments are Vanilla-FFGT and GRPE-FFGT derived from Vanilla Transformer [26] and GRPE [15]. While the number of attention heads is not strictly required to match between the full-range attention module and the focal attention module, we have chosen to keep them consistent. This decision stems from our inability to determine definitively whether global or local information holds greater significance. Furthermore, when comparing with the fully-connected GTs (i.e. replace focal attention module with another full-range attention module with equal number of attention heads), we maintain the total number of attention heads unchanged (e.g. if a FFGT model has 4 focal attention heads and 4 full-range attention heads, its corresponding fully connected GT will possess 8 full-range attention heads).

For hyperparameters, in order to investigate whether our hybrid mechanism of full-range and focal attention outperforms fully connected layers, and to compare the differences in using different attention mechanisms within FFGT, we mandate that the Vanilla, Vanilla-FFGT, GRPE, and GRPE-FFGT maintain consistency in their major model parameters (e.g. number of layers, hidden dimension, and attention heads). Given that Vanilla Transformer and GRPE detail their model hyperparameters for some of the datasets we utilize, we intentionally opted for their configurations. For those where hyperparameters are missing in previous literatures, we mainly followed the choice of GraphGPS [10]. To determine the choice of focal length (FL), we search the parameter space and make the final decision based on validation performance.

The final hyperparameters are presented in Tables 8, 9. In all our experiments, we used AdamW [49] optimizer, with the default setting of $\beta_1 = 0.9$, $\beta_2 = 0.999$ and $\epsilon = 10^{-8}$, together with linear "warm-up" and linear learning rate decay.

All experiments are run on a laptop with AMD Ryzen 9 5950X 16-Core processor, 64.0 GB RAM and one Nvidia RTX3090ti GPU.

Table 8: Hyperparameters of Vanilla-FFGT for 5 graph-level datasets

Hyperparameter	ZINC	MolPCBA	Peptides-func	Peptides-struct	SBM-Pattern
# Layers	12	8	4	4	6
Hidden dim	80	304	120	120	80
# FocalAttn Heads	4	4	2	2	2
# FullAttn Heads	4	4	2	2	2
# Focal Length	1	3	4	4	-
Dropout	0.1	0.1	0.1	0.1	0.1
Attention dropout	0.1	0.3	0.3	0.3	0.1
Positional Encoding	LapPE-8	LapPE-8	LapPE-10	LapPE-10	LapPE-8
PE dim	8	8	10	10	8
PE encoder	linear	linear	linear	linear	linear
Batch size	256	64	32	32	32
Learning Rate	2e-4	2e-4	2e-4	1.2e-4	2e-4
# Epochs	5000	80	250	250	100
# Warmup epochs	500	5	10	10	5
Weight decay	0.001	0.001	0.001	0.001	0.001
# Parameters	494k	7.9M	468k	468k	334k

Table 9: Hyperparameters of GRPE-FFGT for 4 graph-level datasets

Hyperparameter	ZINC	MolPCBA	Peptides-func	Peptides-struct
# Layers	12	8	4	4
Hidden dim	80	304	120	120
# FocalAttn Heads	4	4	2	2
# FullAttn Heads	4	4	2	2
# Focal Length	1	3	4	4
Max hop	5	5	20	20
Dropout	0.1	0.1	0.1	0.1
Attention dropout	0.1	0.3	0.3	0.3
Batch size	256	64	32	32
Learning Rate	2e-4	2e-4	3e-4	3e-4
# Epochs	5000	80	250	250
# Warmup epochs	500	5	10	10
Weight decay	0.001	0.001	0.001	0.001
# Parameters	483k	7.8M	452k	452k

Table 10: Hyperparameters of GRPE-FFGT for 3 node-level datasets

Hyperparameter	Cora	CiteSeer	Chameleon
# Layers	3	3	4
Hidden dim	120	120	120
# FocalAttn Heads	4	4	4
# FullAttn Heads	4	4	4
# Focal Length	1	1	1
Max hop	4	4	3
Dropout	0.3	0.3	0.3
Attention dropout	0.5	0.5	0.5
Learning Rate	1e-3	1e-3	1e-3
# Epochs	100	100	100
# Warmup epochs	5	5	5
Weight decay	0.001	0.001	0.001